Electronic Supplementary Material (ESI) for Dalton Transactions.

Supplementary Information

Sulfur hetero atoms based MOFs with long-last room-temperature phosphorescence and high photoelectric response

Xiao-Gang Yang,[a] Zhi-Min Zhai,[ac] Xin-Yi Liu,[a] Jin-Yao Li,[a] Fei-Fei Li,*[b] and Lu-Fang Ma*[ac]

[a]College of Chemistry and Chemical Engineering, Henan Key Laboratory of Function-Oriented Porous Materials, Luoyang Normal University, Luoyang 471934, P. R. China
[b]College of Chemistry and Chemical Engineering, Henan Polytechnic University, Jiaozuo, 454000, P. R. China
[c]College of Chemistry, Zhengzhou University, Zhengzhou, 450001, P. R. China.

A. Experimental Section.

1. Materials and general procedures. All chemicals were purchased from commercial provider and used without further purification. Single-crystal X-ray diffraction data for 1 and 2 were collected at normal temperature on an Oxford Diffraction SuperNova area-detector diffractometer using mirror optics monochromated Mo Kα radiation (λ = 0.71073 Å). CrysAlisPro was used for the data collection, data reduction and empirical absorption correction.[1] The crystal structure was solved by direct methods, using SHELXS-2014 and least-squares refined with SHELXL-2014 using anisotropic thermal displacement parameters for all non-hydrogen atoms.[2] The dimethylamine cations were disordered and could not be located. The diffuse electron densities in the structure were therefore treated using the SQUEEZE routine in the program PLATON. The crystallographic data for 1 and 2 were listed in Table S1.

PXRD patterns were collected on a Bruker D8-ADVANCE X-ray diffractometer with Cu *Kα* radiation (λ = 1.5418 Å). Measurements were made in a 2θ range of 5−50° at room temperature with a step of 0.02° (2θ) and a counting time of 0.2 s/ step. The operating power was 40 KV, 40 mA. Room temperature photoluminescence (PL) spectra and time-resolved lifetime were conducted on an Edinburgh FLS1000 fluorescence spectrometer equipped. The fluorescent and phosphorescent spectrums were measured by xenon arc lamp (Xe900) and a microsecond flash lamp, respectively. The time-resolved phosphorescent decay curves were detected by a microsecond flash lamp with 100 Hz for TDA, dps and 2, 50 Hz for 1.

Optoelectronic measurements were performed with a CHI 660E electrochemical analyzer (CH Instruments, Chenhua Co., Shanghai, China) in a standard three-electrode system using 1 and 2 powder modified indium tin oxide (ITO) glass as the working electrodes with a working area of 1.0 cm^2, a platinum wire electrode as a counter electrode, Ag/AgCl as a reference electrode, and 0.5 M Na_2SO_4 aqueous solution as the electrolyte. The system was conducted in a quartz glass reactor ca. 50 cm^3, and irradiated by a 300 W xenon lamp. Transient current density-time characteristics was tested at bias potential of 0, -0.2 and -0.4 V vs. Ag/AgCl, respectively.

2. Synthesis of 1 and 2

Synthesis of $[Zn_{3.5}(TDA)_4(DMF)_3](Me_2NH_2)$ (1). A mixture of TDA (TDA= 2,5-thiophene dicarboxylic acid, 0.086 g, 0.5 mmol), $Zn(NO_3)_2{\cdot}6H_2O$ (0.297 g, 1 mmol), and DMF (8 mL) was placed in Teflon-lined stainless steel vessels, heated to 120 ℃ for 2 days, and then cooled to room temperature over 24 h. Colorless block crystals of 1 was obtained. In 1, the protonated dimethylamine $(Me_2NH_2)^+$ counter ions were generated from the decomposition of DMF.

Synthesis of [Zn(TDA)(dps)] (2). A mixture of TDA (TDA= 2,5-thiophene dicarboxylic acid, 0.0172 g, 0.1 mmol), dps (dps= 4,4'-dipyridine sulfide, 0.0188 g, 0.1 mmol), $Zn(NO_3)_2{\cdot}6H_2O$ (0.0595 g, 0.2 mmol), KOH (0.0112 g, 0.2 mmol), and H_2O (8 mL) was placed in Teflon-lined stainless steel vessels, heated to 120 ℃ for 3 days, and then cooled to room temperature over 24 h. Light yellow block crystals of 2 was obtained.

Preparation of working electrode. The as-synthesized crystals (10 mg) of 1 and 2 were grinded to powder and then dispersed in 2 mL of ethanol solution by ultrasonication to form a homogeneous slurry. Finally, daubed the appropriate amount sample evenly over 1 cm^2 of area on a piece of 1 cm × 4 cm ITO and dried at room temperature for measurements.

3. Electronic structure calculations

All calculations were performed with the periodic density functional theory (DFT) method using Dmol^3 module in Material Studio software package.[3] The initial configuration was fully optimized by Perdew-Wang (PW91) generalized gradient approximation (GGA) method with the double numerical basis sets plus polarization function (DNP).[4-6] The core electrons for metals were treated by effective core potentials (ECP). The self-consistent field (SCF) converged criterion was within 1.0×10^{-5} hartree atom^{-1} and the converging criterion of the structure optimization was 1.0×10^{-3} hartree bohr^{-1}. The Brillouin zone is sampled by $1 \times 1 \times 1$ k-points, and test calculations reveal that the increase of k-points does not affect the results.

B. Supporting Figures

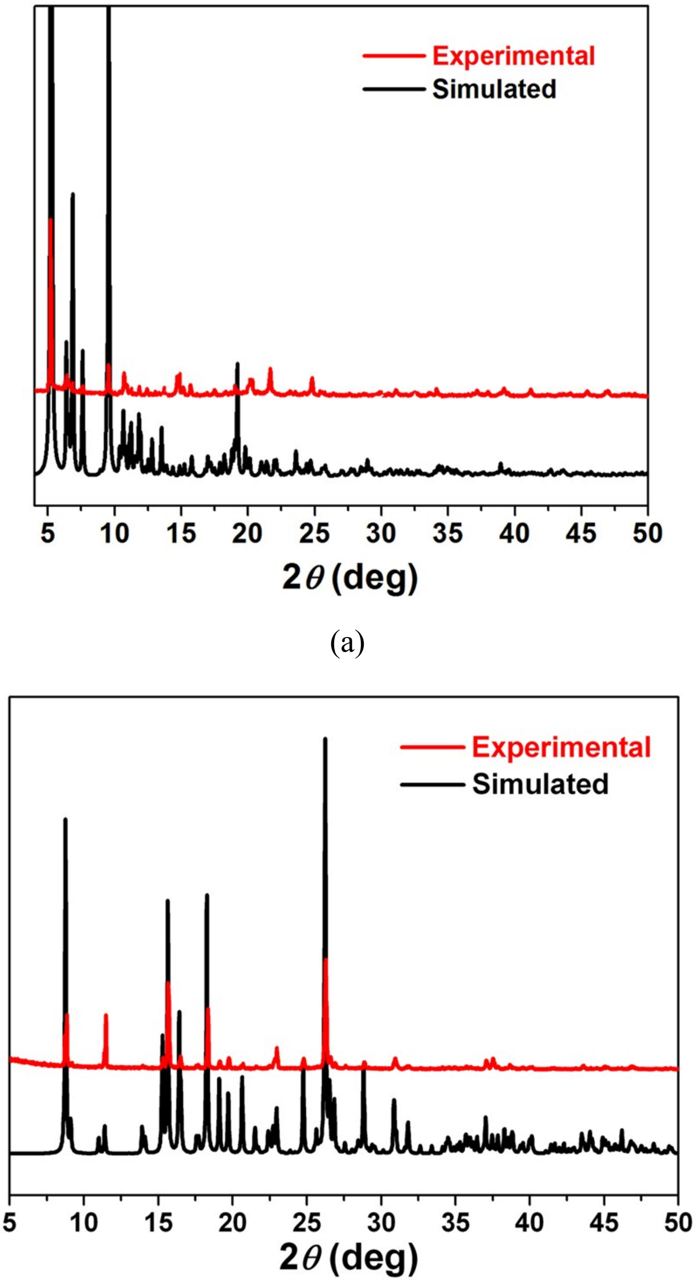

(a)

(b)

Figure S1. PXRD patterns of 1 (a) and 2 (b).

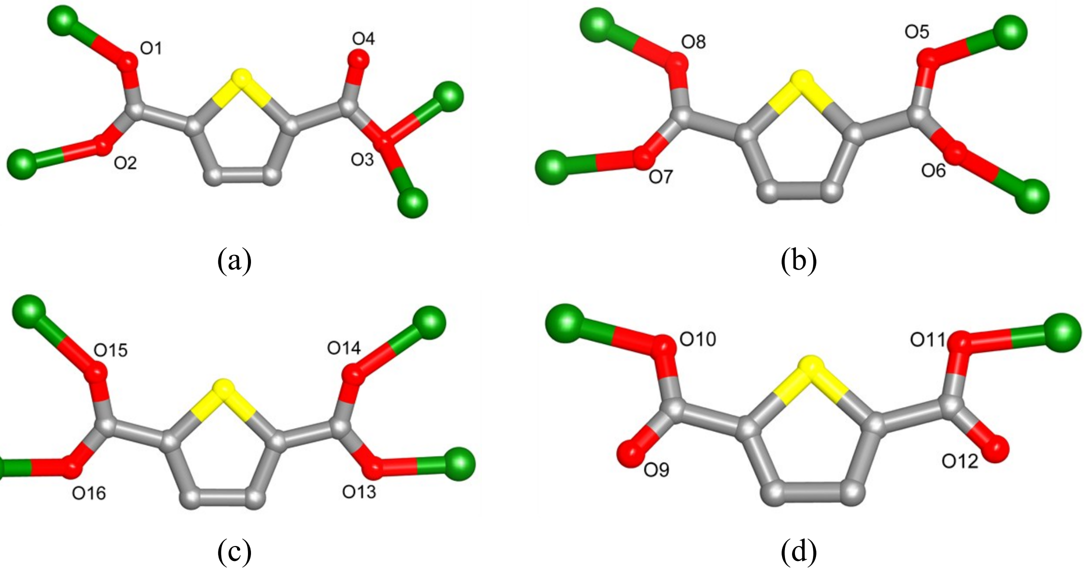

(a) (b)

(c) (d)

Figure S2. View of the coordination modes of TDA ligand in 1.

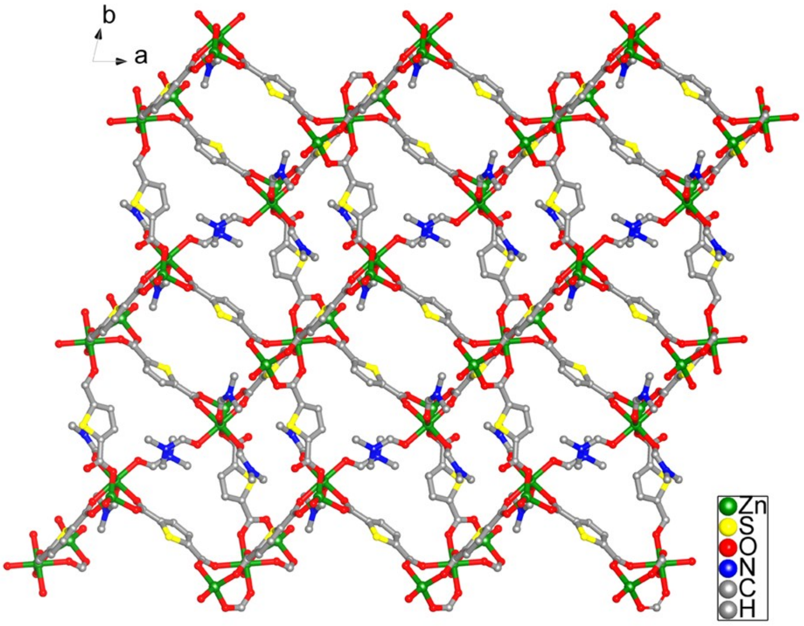

Figure S3. View of the 2D layer in 1 along *ab* plane with coordinated DMF molecules reside in the windows.

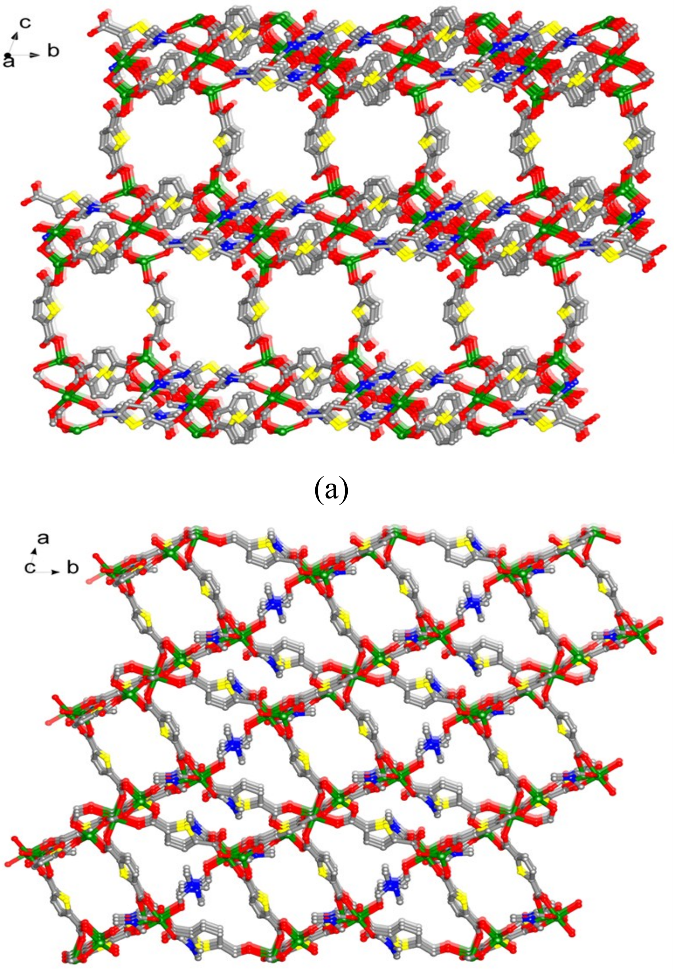

(a)

(b)

Figure S4. View of the 3D network along *a* (a) and *c* (b) direction in 1.

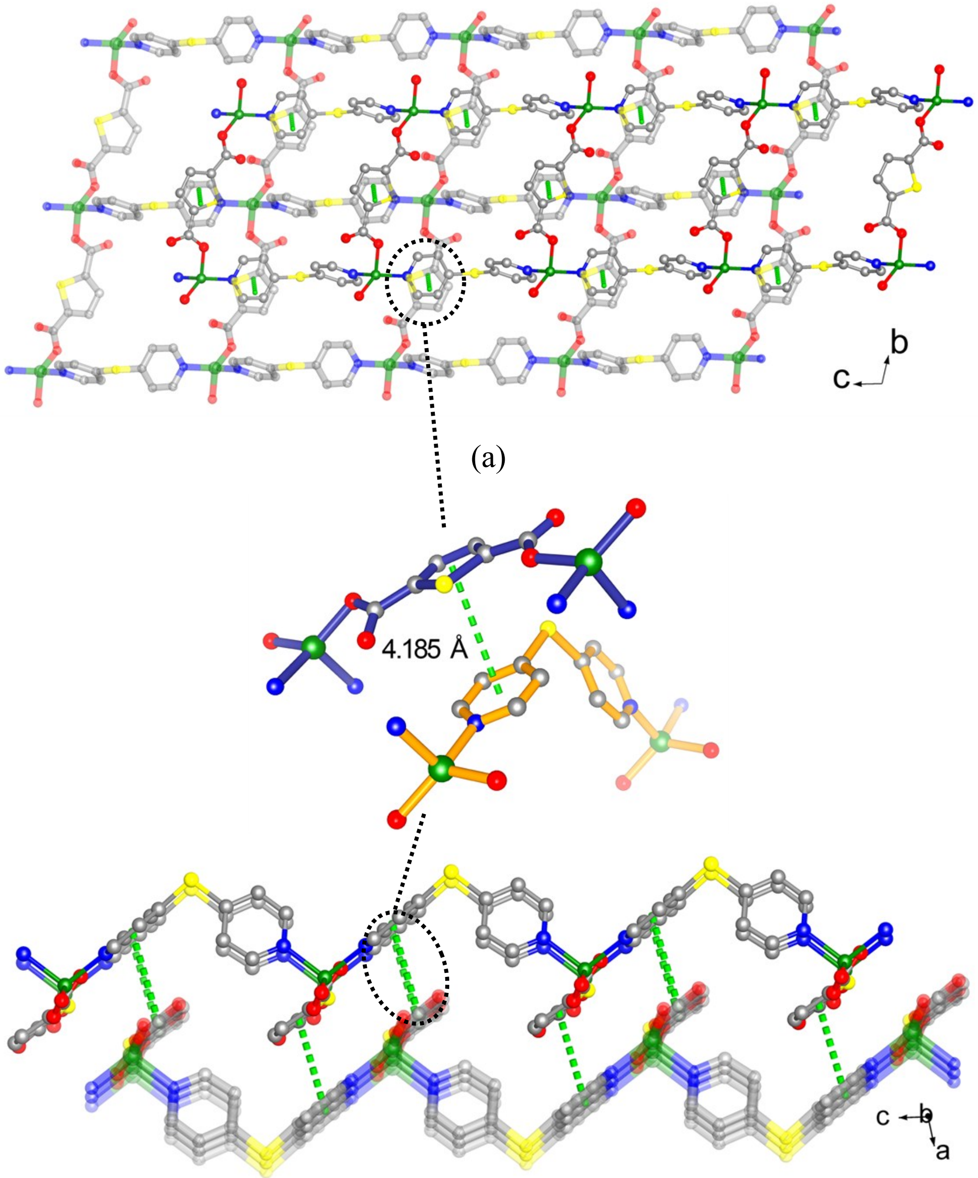

(a)

(b)

Figure S5. View of the π···π stacking interactions between adjacent layers in 2.

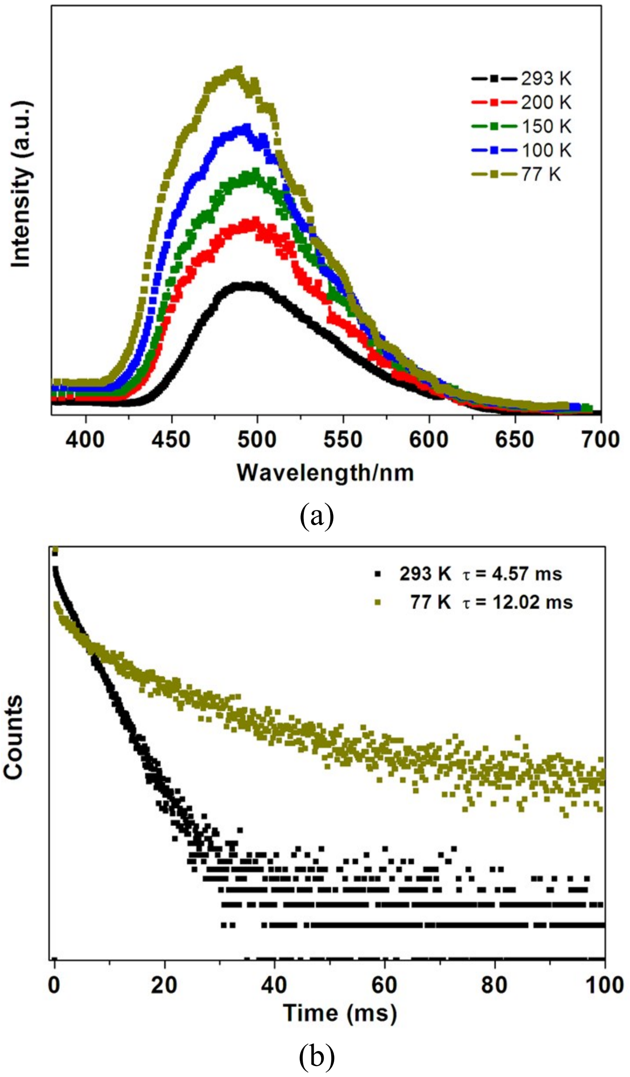

(a)

(b)

Figure S6. (a) Steady-state phosphorescence spectra of 1 measured at temperatures from 293 to 77 K. (b) Time-resolved emission decay curves of 1 at 293 and 77 K.

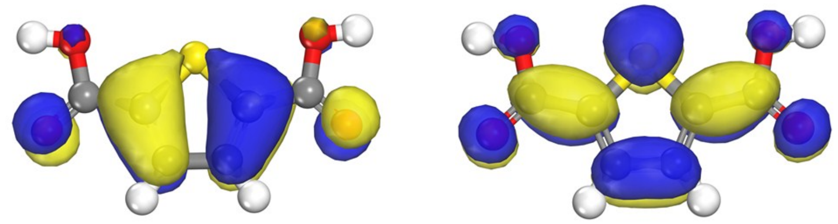

HOMO LUMO

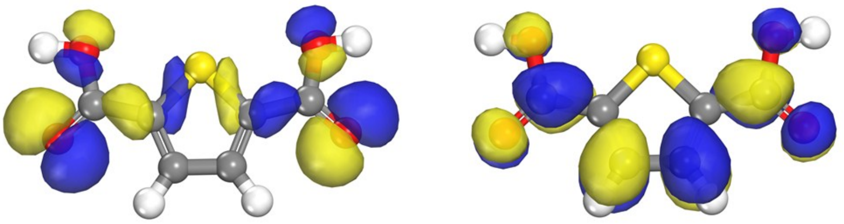

HOMO-1 LUMO+1

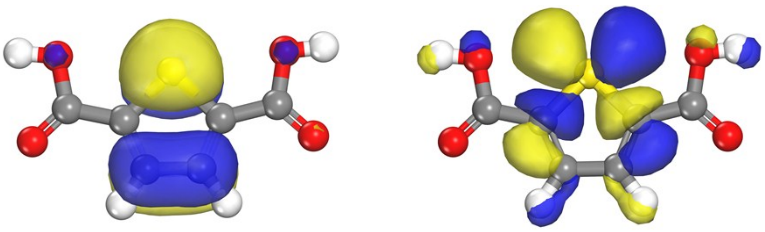

HOMO-2 LUMO+2

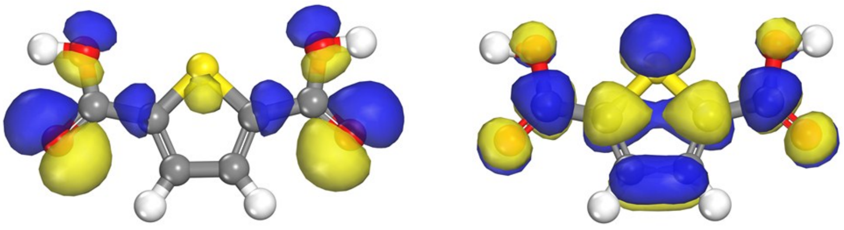

HOMO-3 LUMO+3

Figure S7. The distributions of highest occupied molecular orbitals (HOMO) and lowest unoccupied molecular orbitals (LUMO) of TDA.

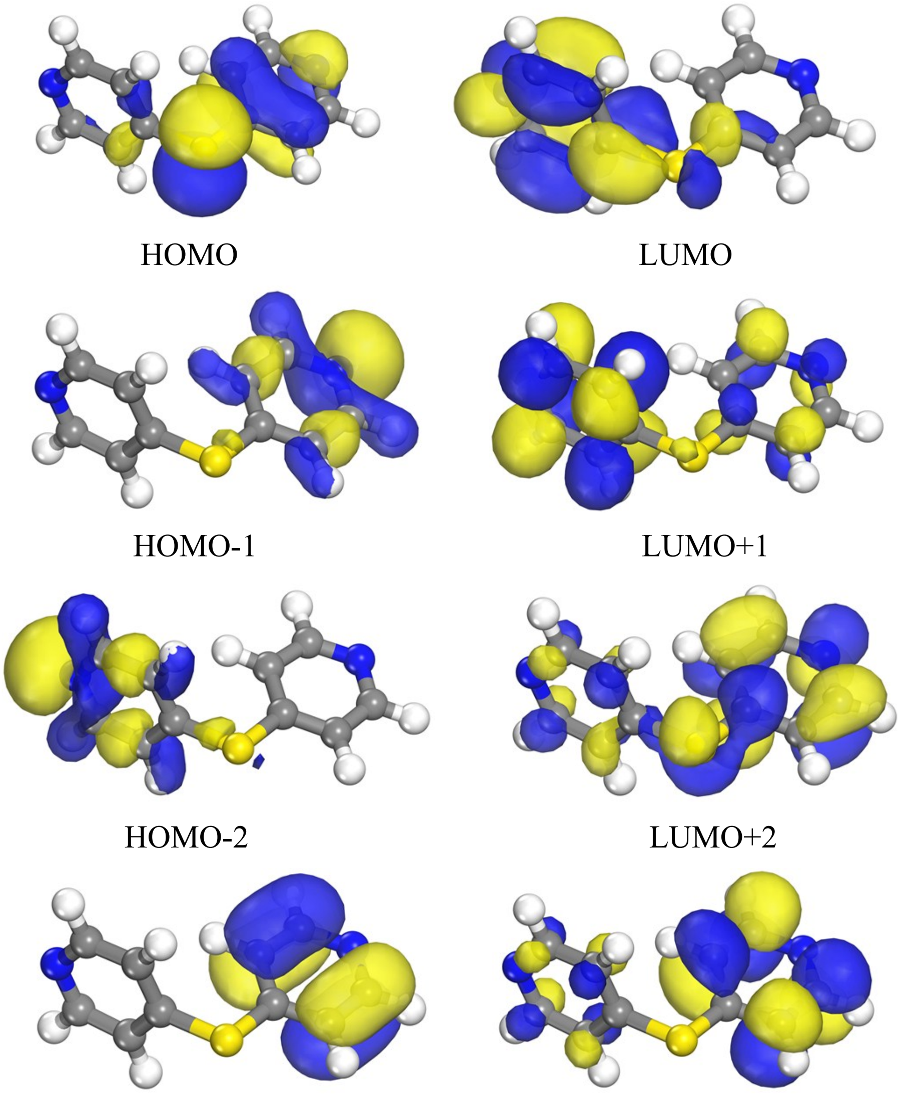

HOMO LUMO

HOMO-1 LUMO+1

HOMO-2 LUMO+2

HOMO-3 LUMO+3

Figure S8. The distributions of highest occupied molecular orbitals (HOMO) and lowest unoccupied molecular orbitals (LUMO) of dps.

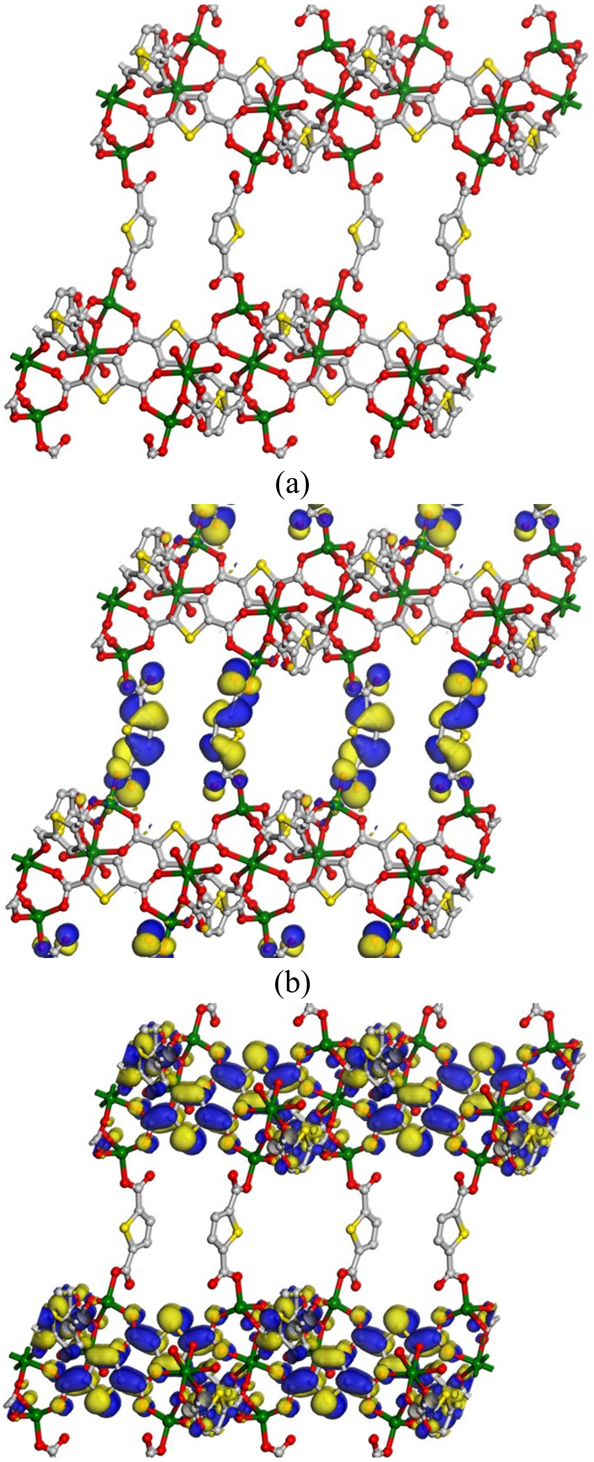

(a)

(b)

(c)

Figure S9. (a) View of the 3D network of 1. (b) and (c) The distributions of highest occupied molecular orbital (HOMO) and lowest unoccupied molecular orbital (LUMO) of 1.

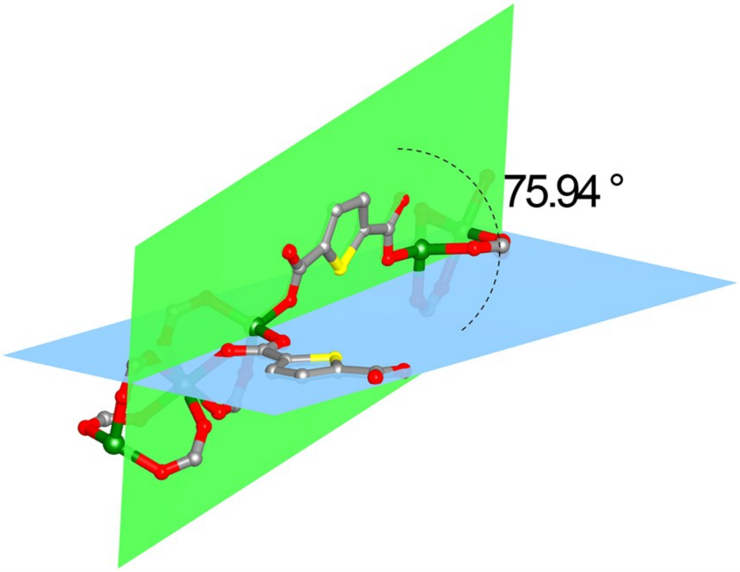

Figure S10. The different arrangement of tetradentate and bidentate TDA ligands with dihedral angles of 75.94 ° in 1.

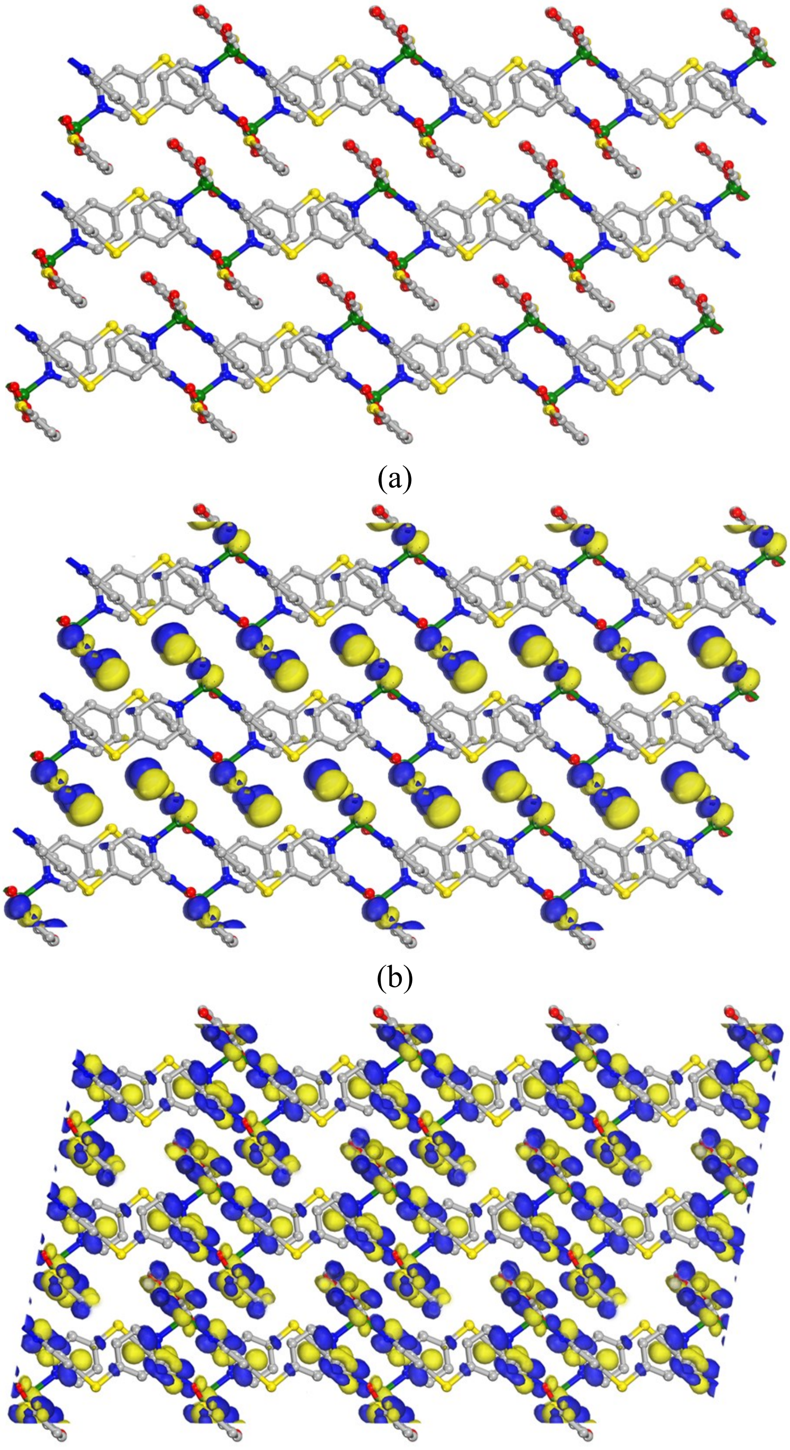

(a)

(b)

(c)

Figure S11. (a) View of the 3D network of 2. (b) and (c) The distributions of highest occupied molecular orbital (HOMO) and lowest unoccupied molecular orbital (LUMO) of 2.

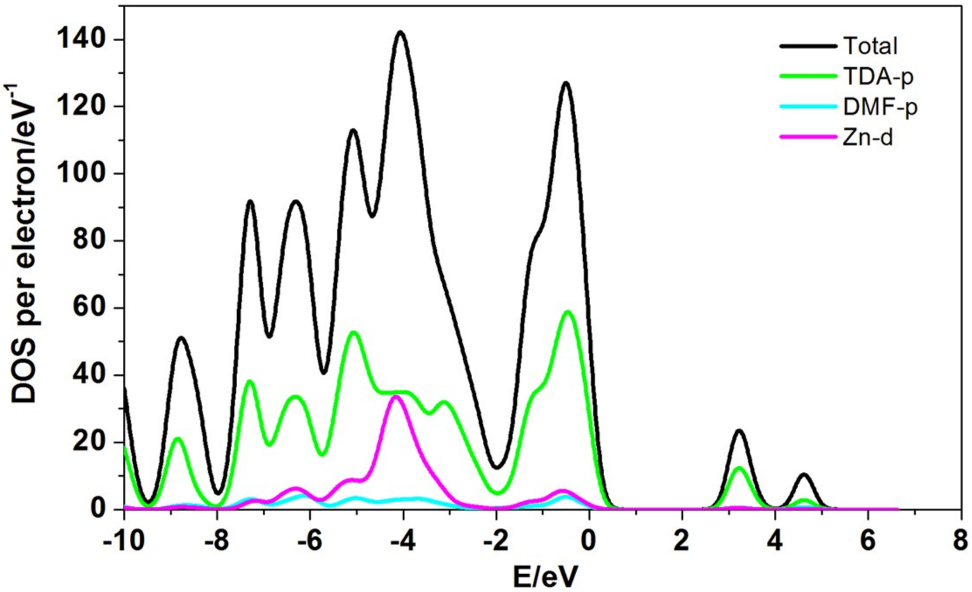

(a)

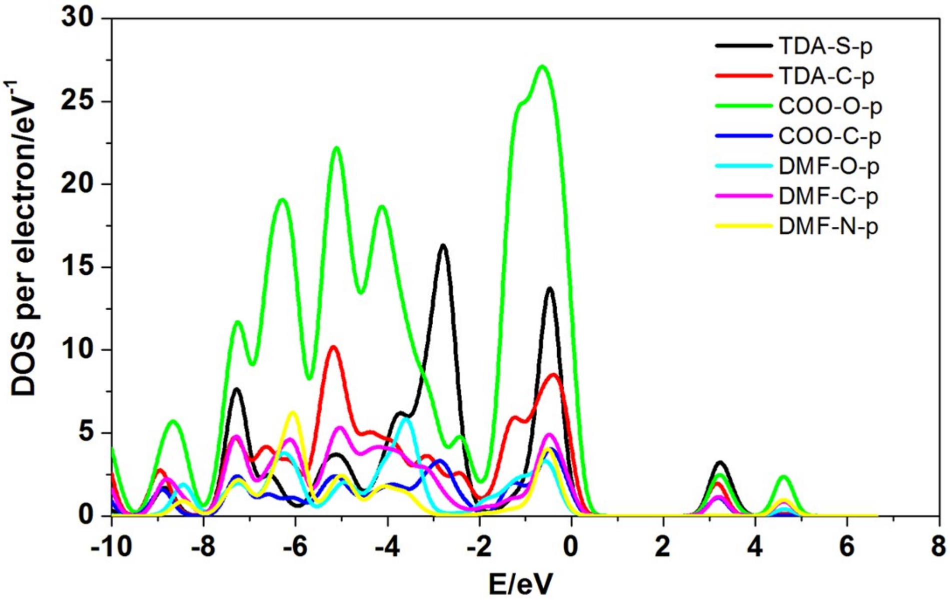

(b)

Figure S12. Total/partial electronic density of state (TDOS and PDOS) for the DFT optimized structure of 1.

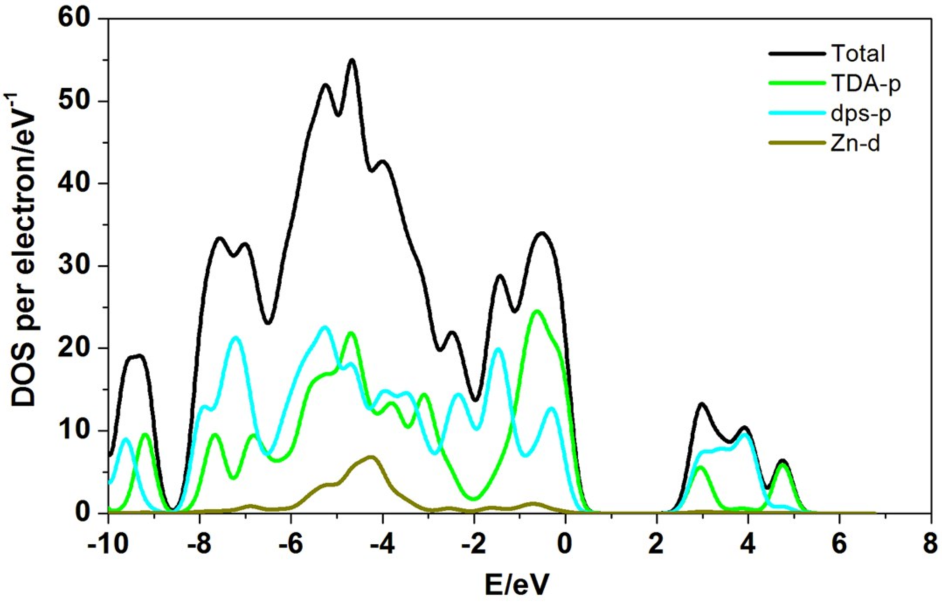

(a)

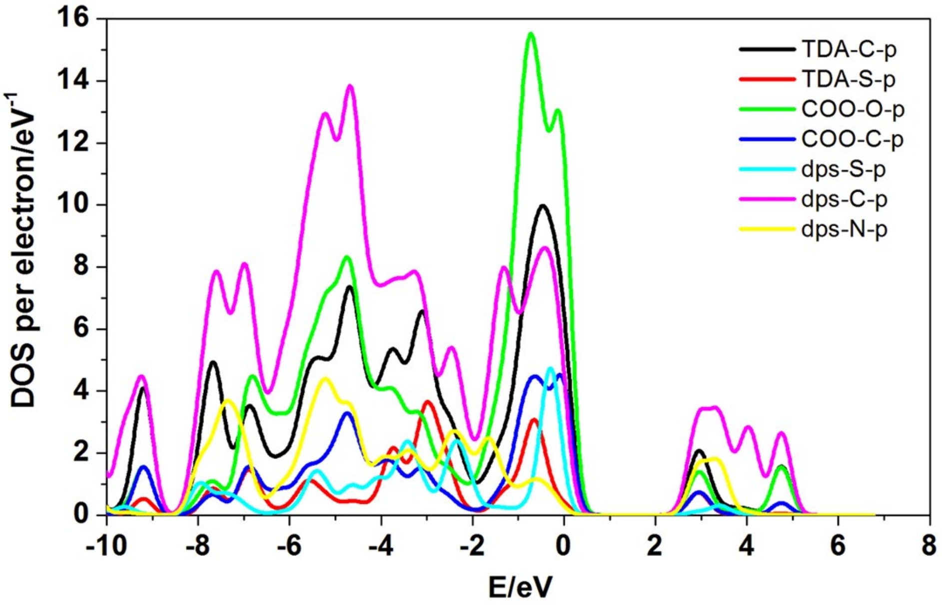

(b)

Figure S13. Total/partial electronic density of state (TDOS and PDOS) for the DFT optimized structure of 2.

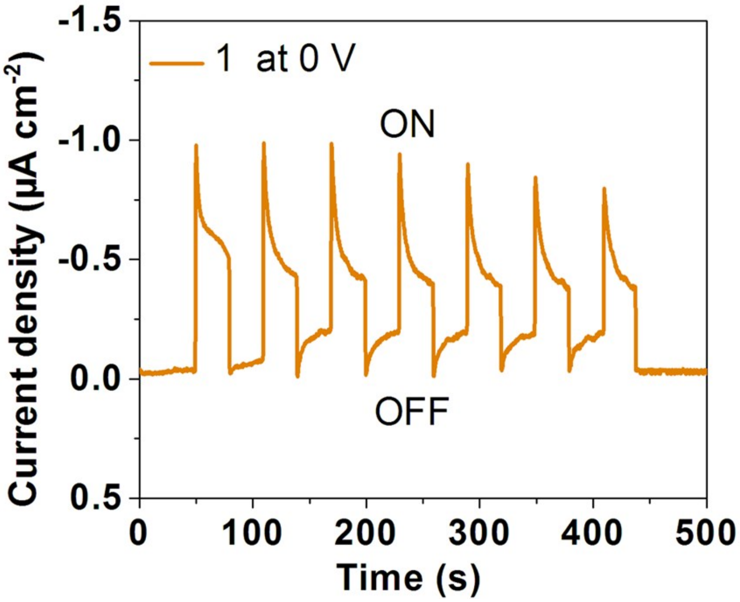

(a)

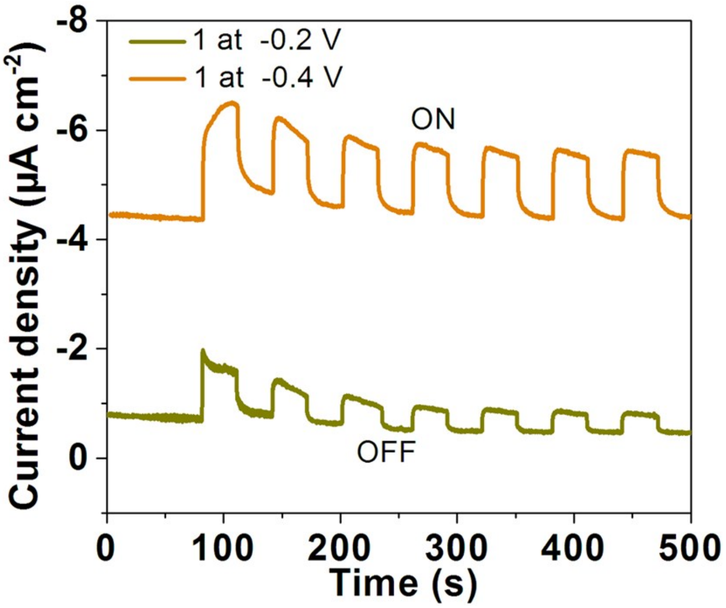

(b)

Figure S14. Transient current density–time curves of 1 at different bias potential of vs. Ag/AgCl in 0.5 M Na_2SO_4.

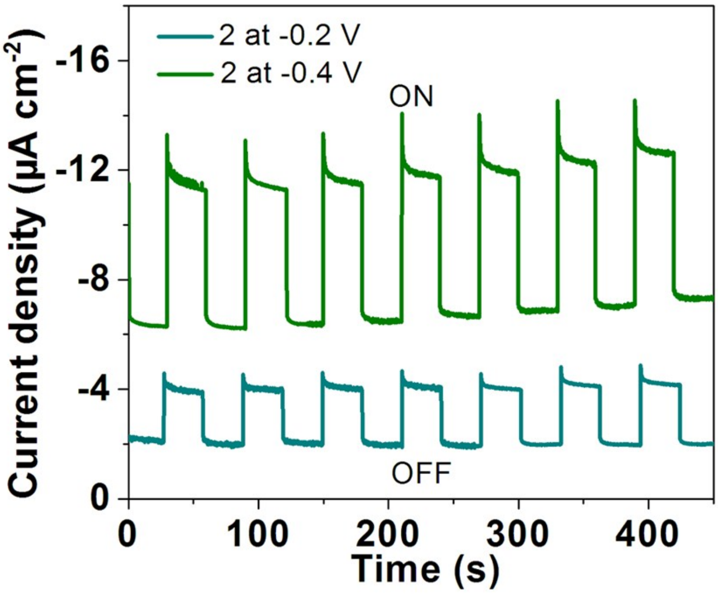

Figure S15. Transient current density–time curves of 2 at different bias potential of vs. Ag/AgCl in 0.5 M Na_2SO_4.

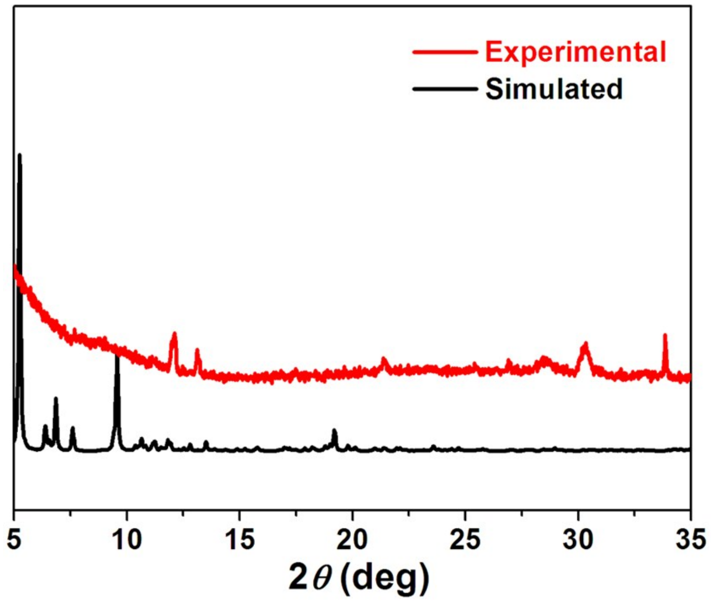

(a)

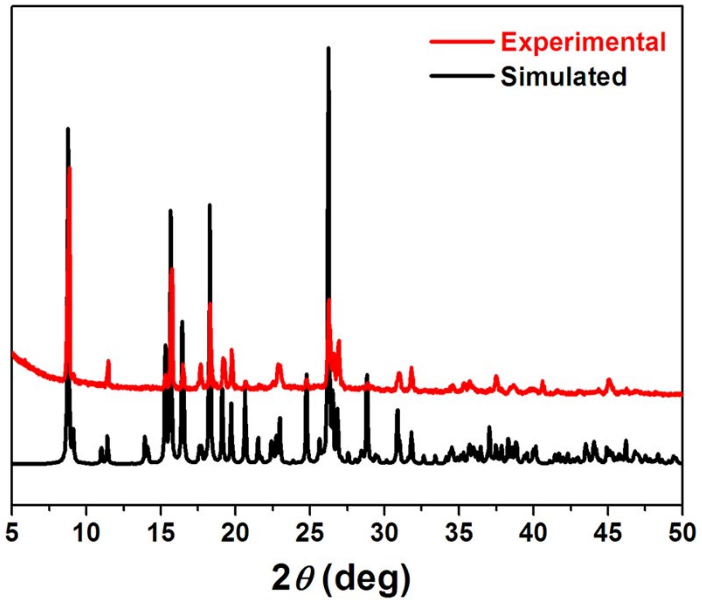

(b)

Figure S16. PXRD patterns of 1 (a) and 2 (b) after photoelectric measurements.

Table S1. Crystallographic data for 1 and 2.

Samples	$[Zn_{3.5}(TDA)_4(DMF)_3]$ (1)	[Zn(TDA)(dps)] (2)
Chemical formula	$C_{33}H_{29}N_3O_{19}S_4Zn_{3.5}$	$C_{16}H_{10}N_2O_4S_2Zn$
Formula weight	1128.63	423.75
CCDC NO.	1958280	1958281
Crystal system	Triclinic	Triclinic
Space group	$P\bar{1}$	$P\bar{1}$
a (Å)	15.4577(9)	7.9030(4)
b (Å)	16.9810(11)	10.0174(7)
c (Å)	19.2095(12)	10.5515(8)
α (°)	66.763(6)	103.392(6)
β (°)	66.652(6)	99.731(5)
γ (°)	69.687(5)	92.961(5)
V (Å^3)	4143.6(5)	797.33(9)
Z	2	2
D (g cm^{-3})	0.905	1.765
μ (mm^{-1})	1.144	1.827
R_{int}	0.0865	0.0296
Goof	1.060	1.030
$R_1{}^a$ ($I>2\sigma(I)$)	0.0922	0.0384
$wR_2{}^a$ ($I>2\sigma(I)$)	0.2536	0.0776

^{a} $R_1 = \Sigma(||F_o| - |F_c||)/\Sigma|F_o|$; ^{b} $wR_2 = [\Sigma w(|F_o|^2 - |F_c|^2)^2/\Sigma w(F_o{}^2)^2]^{1/2}$

D. Supporting References

1 CrysAlisPro, Rigaku Oxford Diffraction, Version 1.171.39.6a.

2 (*a*) G. M. Sheldrick, A short history of SHELX. *Acta Crystallogr. Sect. A*., 2008, **A64**, 112–122. (*b*) G. M. Sheldrick, SHELXT–Integrated space-group and crystal-structure determination. *Acta Cryst*., 2015, **A71**, 3–8.

3 B. Delley, An all-electron numerical method for solving the local density functional for polyatomic molecules. *J. Chem. Phys*., 1990, **92**, 508–517.

4 Dmol^3 Module, MS Modeling, Version 2.2; Accelrys Inc.: San, Diego, 2003.

5 B. Delley, From molecules to solids with the DMol^3 approach. *J. Chem. Phys*., 2000, **113**, 7756–7764.

6 J. P. Perdew, J. A. Chevary, S. H. Vosko, K. A. Jackson, M. R. Pederson, D. J. Singh, C. Fiolhais, Atoms, molecules, solids, and surfaces: Applications of the generalized gradient approximation for exchange and correlation. *Phys. Rev. B*., 1992, *46*, 6671–6687.